Carbohydrate Polymers 84 (2011) 1126–1132

Contents lists available at ScienceDirect

Carbohydrate Polymers

journal homepage: www.elsevier.com/locate/carbpol

Chitosan rods reinforced by aligned multiwalled carbon nanotubes via magnetic-field-assistant *in situ* precipitation

Zhengke Wang[a], Hui Zhao[a], Li Fan[b], Jun Lin[b], Pengyu Zhuang[a], Wang Zhang Yuan[a,c], Qiaoling Hu[a,*], Jing Zhi Sun[a,**], Ben Zhong Tang[a,c,***]

[a] *Institute of Biomedical Macromolecules, Department of Polymer Science and Engineering, Key Laboratory of Macromolecule Synthesis and Functionalization, Ministry of Education, Zhejiang University, Hangzhou 310027, China*
[b] *The First Affiliated Hospital, Zhejiang University, Hangzhou 310003, China*
[c] *Department of Chemistry, The Hong Kong University of Science & Technology, Clear Water Bay, Kowloon, Hong Kong, China*

ARTICLE INFO

Article history:
Received 23 August 2010
Received in revised form
23 December 2010
Accepted 4 January 2011
Available online 8 January 2011

Keywords:
Chitosan
Multiwalled carbon nanotubes
Poly(*p*-amino-phenylacetylene)
Magnetism
Alignment
Biomaterials

ABSTRACT

Chitosan (CS) rods are a good candidate as temporary mechanical supports in bone regeneration, however the bending strength and bending modulus should be improved to match commercially available devices used for bone fracture internal fixation. Poly(*p*-amino-phenylacetylene)/multi-walled carbon nanotubes (PaPA/MWCNTs) hybrids with superparamagnetic Fe_3O_4 nanoparticles (Fe_3O_4@PaPA/MWCNTs) are applied to reinforce the CS rods. Fe_3O_4@PaPA/MWCNTs could be uniformly dispersed in CS solution and aligned by an external magnetic field, in the direction parallel to the axis of CS rod. This greatly helped to resist the bending stress, thus the bending strength and modulus of the reinforced CS rods are 124.6 MPa and 5.3 GPa, respectively; which are 34.8% and 29.3% stronger than pure CS rods. As a result, the magnetic-field-assisted *in situ* precipitation method offers one feasible route for the reinforcement of CS-based devices with nano-scaled one-dimensional additives such as MWCNTs. In addition, CS-based biomaterials containing Fe_3O_4@PaPA/MWCNTs could obviously promote MG63 cells proliferation, so CS rods modified with Fe_3O_4@PaPA/MWCNTs are good candidates for bone fracture internal fixation.

1. Introduction

Chitosan (CS) has been widely used as temporary mechanical supporter for the regeneration of bone due to its desirable biocompatibility, biodegradability and inherent wound healing properties (Di Martino, Sittinger, & Risbud, 2005; Gupta & Jabrail, 2006; Kim et al., 2004; Leroux, Hatim, Freche, & Lacout, 1999; Moroni & Elisseeff, 2008; Zhu, Wang, Cui, Feng, & De Groot, 2003). But its solubility and processability are undesirable due to the multiple hydrogen-bonds linking between polysaccharide macromolecules. Protonation of the amino groups in the polysaccharide and breaking of the hydrogen bonding make CS soluble in acidic aqueous solution. When treated with basic aqueous solution, the acidic CS solution is neutralized and the polysaccharide macromolecules recover to their primary state. By gradually soaking NaOH aqueous solution into CS solution holding in a cylindrical mold, we prepared pure CS rods and CS/hydroxyapatite composite rods (Hu, Qian, Li, & Shen, 2003). This strategy is referred as an *in situ* precipitation, which provides a simple method to fabricate CS-based devices in various shapes and dimensions (Chen, Hu, Chen, Li, & Shen, 2006; Hu et al., 2003; Hu, Chen, Li, & Shen, 2006; Hu, Li, Wang, & Shen, 2004). In average, the bending strength and modulus of the pure CS rods made by *in situ* precipitation are 92.4 MPa and 4.1 GPa, respectively (Hu et al., 2003, 2004). The bending strength is lower than the quota for internal fixation of bone fracture in clinical application. For example, the bending strength and bending modulus of the commercial nails produced by Dikfix are 130 MPa and 2.0–3.0 GPa, respectively (Hu et al., 2002). In the purpose of using the CS rods for the internal fixation of bone fracture, a substantial reinforcement of the pure CS rods have to be realized.

Multiwalled carbon nanotubes (MWCNTs) have found important applications in high-performance composites due to their extraordinary tensile strength (Dresselhaus, Dresselhaus, & Eklund, 1996; Saito, Dresselhaus, & Dresselhaus, 1998). The properly surficial modified MWCNTs have shown to be biocompatible and demonstrated potential usages in the area of tissue engineering

* Corresponding author. Tel.: +86 571 8795 3726; fax: +86 571 8795 3726.
** Corresponding author. Tel.: +86 571 87953734; fax: +86 571 8795 3734.
*** Corresponding author at: Institute of Biomedical Macromolecules, Department of Polymer Science and Engineering, Key Laboratory of Macromolecule Synthesis and Functionalization, Ministry of Education, Zhejiang University, Hangzhou 310027, China.
E-mail addresses: huql@zju.edu.cn (Q. Hu), sunjz@zju.edu.cn (J.Z. Sun), tangbenz@ust.hk (B.Z. Tang).

0144-8617/$ – see front matter © 2011 Elsevier Ltd. All rights reserved.
doi:10.1016/j.carbpol.2011.01.001

and drug delivery systems (Hussain et al., 2009; Nel et al., 2009; Saito et al., 2008, 2009; Sirivisoot & Webster, 2008; Veetil & Ye, 2009). Meanwhile, recent investigation of the response of bone cells to MWCNTs indicated that MWCNTs inhibit osteoclastic bone resorption *in vivo* and suppressed a transcription factor essential for osteoclastogenesis *in vitro*. These experimental data suggest that MWCNTs have beneficial effects on bone growth (Narita et al., 2009; Xu, Khor, Sui, & Chen, 2009). As a result, it is rational to recognize that MWCNTs may also be used to reinforce CS rods.

The first premise to make use of MWCNTs in the reinforcement of CS rods is to make the MWCNTs uniformly dispersible in aqueous media because MWCNTs themselves are known to be insoluble in any solvents. Fortunately, some strategies, both covalent and non-covalent surface modification have been developed for effective dispersing MWCNTs in aqueous solutions (Islam, Rojas, Bergey, Johnson, & Yodh, 2003; Kang et al., 2009; Kharisov, Kharissova, Gutierrez, & Mendez, 2009; Lee, Kim, Chen, Shao-Horn, & Hammond, 2009; MacNeil, 2008; Matarredona et al., 2003; Peng & Wong, 2009; Yurekli, Mitchell, & Krishnamoorti, 2004). In our previous research, we found that poly(phenylacetylene) (PPA) and its derivatives containing aromatic pendants such as pyrene, ferrocene and triphenylamine moieties showed strong power to disperse MWCNTs in proper solvents by wrapping PPA chains onto the surface of MWCNTs (Tang & Xu, 1999; Xu et al., 2008; Yuan et al., 2006, 2007; Zhao et al., 2008, 2009). In addition, the amino and carboxylic groups modified PPAs could even lead to desirable dispersion of MWCNTs in aqueous medium. Noncovalent functionalization of MWCNTs with PPAs is harmless to the inherent mechanical properties of MWCNTs, thereby is helpful to enhance the mechanical strength of CS rods. Moreover, good biocompatibility and cytophilic property of PPAs have been verified by intentionally designed experiments (Salhi et al., 2001).

Alignment of MWCNTs in a specified direction is the second premise to make full use of the intrinsic physical properties of MWCNTs. It is expected that the bending strength and modulus can be enhanced when the MWCNTs are aligned parallel to the axial direction of a CS rod. According to literatures, the orientation of MWCNTs could be realized by different techniques such as using liquid crystals as self-organizing templates (Kumar & Bisoyi, 2007; Lagerwall et al., 2007; Scalia et al., 2008), mechanical drawing (Dou et al., 2006; Miaudet et al., 2005), and electrophoretic deposition (Kim, Xuan, Ye, Mohammadi, & Lee, 2008; Kim, Lee, Tanaka, & Weiss, 2008; Lu, Cheng, Leduc, & Ho, 2008). But for the preparation of CS rods, above-mentioned methods are useless. In the present research, we try the strategy of using magnetic force to induce the alignment of MWCNTs (Tumpane, Karousis, Tagmatarchis, & Norden, 2008). The MWCNTs were firstly coated with poly(*p*-aminophenylacetylene); then magnetic Fe_3O_4 nanoparticles were chemically deposited onto the surface of amino-functionalized PPA/MWCNTs hybrid by the coordination of amino groups to Fe^{2+} and Fe^{3+} cations. The acidic solution containing MWCNTs decorated with Fe_3O_4 nanoparticles and PPA-based polycations were mixed with CS solution. The mixture was filled into a cylindrical mold, which was immersed into a basic solution for *in situ* precipitation. During the precipitation process, an external magnetic field was applied in the axial direction of the cylindrical mold. The alignment of the MWCNTs would be induced by the applied magnetic field.

Finally, Fe_3O_4/NH_2-PPA/MWCNTs-CS nanocomposite rods were fabricated. Moreover, our experimental results demonstrate that the Fe_3O_4/NH_2-PPA/MWCNTs can be uniformly dispersed in CS matrix and the orientation of the Fe_3O_4-deposited MWCNTs can be achieved. Foremost, both the bending modulus and strength of the modified CS rods have been enhanced.

Table 1
Mass ratio of PaPA, $FeCl_2{\cdot}4H_2O$, $FeCl_3{\cdot}6H_2O$ and MWCNTs of Fe_3O_4@PaPA/MWCNTs.

Sample	PaPA (mg)	$FeCl_2{\cdot}4H_2O$ (mg)	$FeCl_3{\cdot}6H_2O$ (mg)	MWCNTs (mg)
Fe_3O_4@PaPA/MWCNTs-1	50	70	140	8
Fe_3O_4@PaPA/MWCNTs-2	100	140	280	16

2. Experimental

2.1. Materials

Chitosan (biomedical grade, $M = 5.63 \times 10^5$, D.D = 91%, Qingdao Haihui Bioengineering Co., Ltd), acetic acid (CP, Yixing Niujia Chemical Reagent Plant), sodium hydroxide (AR, Hangzhou Xiaoshan Chemical Reagent Corporation), MWCNTs (20–30 nm in diameter, ~30 μm in length, Shenzhen Nanotech Port Co., Ltd), $FeCl_2{\cdot}4H_2O$ and $FeCl_3{\cdot}6H_2O$ (AR, Sinopharm Chemical Reagent Co., Ltd), permanent magnet (N-35, 12000G, Ningbo Sanhe Qiangci Co., Ltd). 4-Aminophenylacetylene is commercially available and purchased from Aldrich. The catalyst of $Rh^+(nbd)[C_6H_5B\text{-}(C_6H_5)_3]$ was prepared in our laboratories, where nbd is the abbreviation of 2,5-norbornadiene.

2.2. Preparation of water soluble polymer-MWCNTs hybrids

The synthesis and characterization of poly(*p*-aminophenylacetylene) (PaPA) were carried out in the same procedures as reported in literature (Yuan et al., 2009). PaPA is readily soluble in acidic aqueous solution, and protonated PaPA is derived. Simple mixing the protonated PaPA with MWCNTs afforded polymer/MWCNT nanohybrids with a moderate water solubility.

2.3. Preparation of polymer/MWCNT hybrids decorated with magnetic particles

Into a 100 mL two-necked round-bottomed flask with a stir bar, 20 mL hydrochloric acid aqueous solution (pH < 4) and PaPA was added under stirring; a light yellow–brown solution was obtained. Then, MWCNTs were added into the solution. After stirring for 0.5 h, the mixture was filtered through a cotton filter to remove insoluble MWCNTs. $FeCl_2{\cdot}4H_2O$ and $FeCl_3{\cdot}6H_2O$ were introduced into the filtrate. After stirring for 0.5 h, the pH of the above solution was adjusted to ~12 with sodium bicarbonate aqueous solution, and then adjusted to ~6 with hydrochloric acid aqueous solution. The mass ratio of PaPA, $FeCl_2{\cdot}4H_2O$, $FeCl_3{\cdot}6H_2O$ and MWCNTs of Fe_3O_4@PaPA/MWCNTs is listed in Table 1.

2.4. Preparation of CS-based composite rods containing aligned Fe_3O_4@PaPA/MWCNTs hybrids

180 mL acetic acid aqueous solution (2%, v/v) was added into a 220 mL aqueous solution containing Fe_3O_4@PaPA/MWCNTs nanohybrids. 20 g CS was added into the above mixture; and the stirring was kept for 1 h. A sol of CS containing Fe_3O_4@PaPA/MWCNTs hybrids was obtained. The sol was held for 24 h to remove the trapped air bubbles, and then injected into a cylindrical mold. Put the mold into sodium hydroxide aqueous solution (5%, wt), soaked for 6 h to form CS gel rod containing Fe_3O_4@PaPA/MWCNTs hybrids. During the gel formation process, a pair of permanent magnets was set near the two ends of the mold. The obtained gel rods were washed with deionized water to remove the resultant salts formed in the generation of Fe_3O_4 and the neutralization treatment. Finally, the rods were air-dried in oven at 60 °C, and the dried rods (diameter: 5 mm, length: 10 cm) were sent for structure and property measurements.

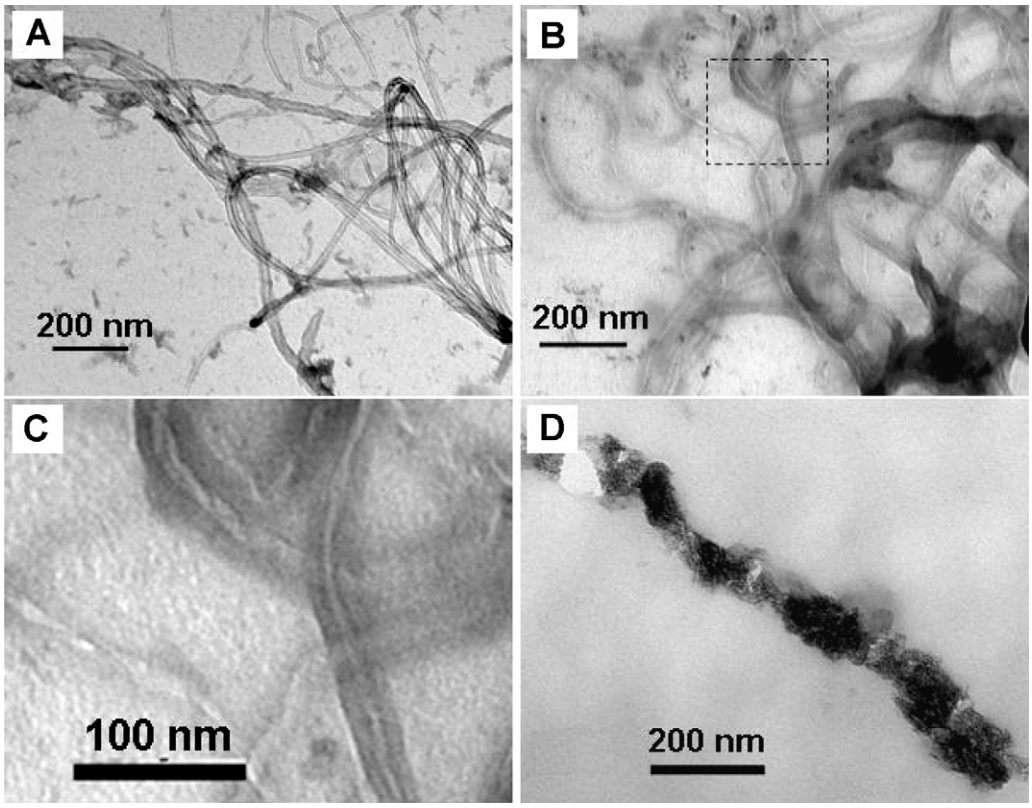

Fig. 1. (A) TEM images of MWCNTs in the primary form, (B) PaPA/MWCNTs hybrids, (C) an amplified image showing the details in dash-lined box of image B, and (D) nano-composite of Fe_3O_4@PaPA/MWCNTs.

2.5. In vitro cell test

CS solution containing Fe_3O_4@PaPA/MWCNTs nanohybrids was casted into membrane, soaked in sodium hydroxide aqueous solution (5%, wt), then washed with deionized water, at last air-dried in oven at 60 °C. The membranes sterilized by ultraviolet irradiation were cut into square pieces (5 mm × 5 mm), and placed in a culture plate. The *in vitro* cell tests of the hybrid membranes were performed using MG63 cells, and the results were compared with those obtained using blank culture plate (control group). MG63 cells were plated at density of 2.5×10^4 cells/mL in 2% FBS DMEM (200 μL). Cultivation was conducted for 24 h, 48 h, 72 h at 37 °C in 5% CO_2. MG63 cells were treated with Cell Titer 96 Aqueous One Solution Reagent (Promeg), and then measured the optical density (OD) with enzyme calibration system (λ = 490 nm, Bio-Rad Model 680) for the cell proliferation assessment.

2.6. Instrumentations

The morphology, dispersion and orientation of MWCNTs in the CS matrix were investigated with TEM (JEOL, Japan, JEM-1200EX) and SEM (Japan, HITACHI S-4800) techniques. The composite rod was cut into ultrathin sections before TEM test, and coated by gold before SEM observation. All of the samples were air-dried in oven at 60 °C for 2 h to remove the moisture before mechanical testing. Bending strength and bending modulus were determined by

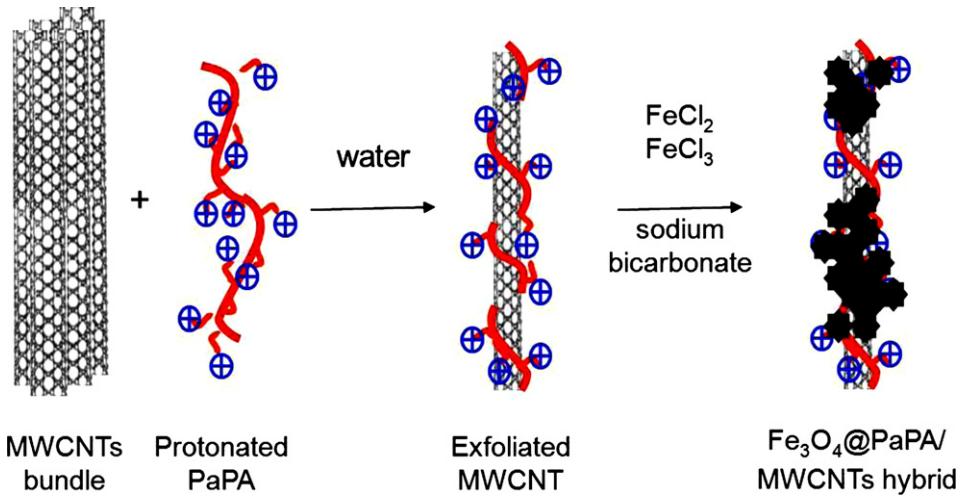

Scheme 1. Preparation route towards Fe_3O_4@PaPA/MWCNTs nanostructures.

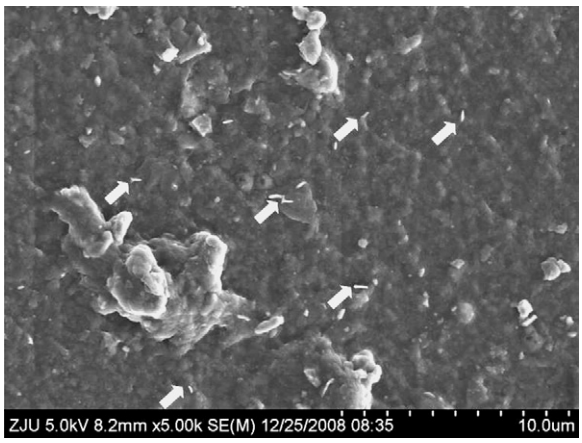

Fig. 2. A typical SEM image showing the morphology of the cross-section of a CS rod containing Fe_3O_4@PaPA/MWCNTs hybrid in CS matrix. The fractured sample was obtained in a mechanical measurement, which was conducted after magnetic-induced alignment. The white arrows direct to the rod-like nanostructures projecting out of the fracture surface.

three-point bending tests, which were performed on the universal materials testing machine made by Reger Company (Shenzhen, China). The span length was 40 mm and loading rate was 2 mm/min. Magnetic measurement was performed by using a magnetometer (Physical Properties Measurement System, PPMS-9, Quantum Design) at 298 K. X-ray diffraction measurement was carried out on Rigaku D/max 2550PC using a monochromatic Cu K_α radiation generated at 40 kV, 300 mA. The samples were scanned from 5° to 60° at a rate of 10°/min.

3. Results and discussion

3.1. Hybridization of CS and Fe_3O_4@PaPA/MWCNTs nanostructure

The wrapping of PaPA polymer chains onto the surface of MWCNTs was experimentally confirmed by our previous investigation, which afforded the solubility of the PaPA/MWCNTs hybrids in organic solvents (Yuan et al., 2009). After treated with acid, the protonated PaPA bestowed the PaPA/MWCNTs hybrid with a proper solubility in aqueous solution. Here, we present the typical morphology of MWCNT used in the construction of nanohybrids. As shown in Fig. 1A, the average diameter of the "naked" MWCNTs is about 20–25 nm, which is in agreement with the product description of MWCNTs. After hybridization with PaPA, the average diameter of the nano-tubular entities becomes 60–70 nm. On the surface of MWCNTs, a thin coating layer can be observed, and the thickness of the coating layer with lower contrast is about 25–30 nm (Fig. 1B and C), which is assigned to PaPA component. Thanks to the amino groups of PaPA, the PaPA/MWCNTs hybrid was bestowed with the solubility up to 316 mg/L in acidic aqueous solutions (see Scheme 1) (Yuan et al., 2009). Upon the protonation of the amino groups, the ionized coating layer not only greatly helps to the exfoliation of the MWCNTs from the bundles, but also effectively prohibits the re-aggregation the separated MWCNTs via static electric repulsion.

As reflected by our previous work, the hybrids of PaPA/MWCNTs were facilely decorated by metal (Ag) and metal oxide (ZnO) nanoparticles, owning to the interaction between amino groups and metal cations (Xu et al., 2007, 2008; Yuan et al., 2009). Similarly, the interaction between amino groups and ferric cations also worked in the formation of Fe_3O_4 nanoparticles on the surface of PaPA/MWCNTs hybrids, furnishing three-component composites of Fe_3O_4@PaPA/MWCNTs (see Scheme 1). By controlling the reaction time and the concentration of the reactants, the loading rate of Fe_3O_4 onto PaPA/MWCNTs can be tuned. As shown in Fig. 1D, the decoration of Fe_3O_4 on the surface of PaPA/MWCNTs hybrid is indiscrete, and the uncovered protonated PaPA segments (polycations) help to solvate the composite of Fe_3O_4@PaPA/MWCNTs. Consequently, the three-component composite can be still partially dissolved in acidic aqueous solutions. Taking the advantage of this solubility, the Fe_3O_4@PaPA/MWCNTs hybrid can be uniformly dispersed in CS solution and kept separating through the *in situ* precipitation process. The SEM image in Fig. 2 demonstrates the morphology of the cross-section of the fracture that spontaneously formed in the mechanical measurement. The arrows direct to the rod-like nanostructures projecting out of the fracture surface, which can be assigned to the hybrid nanotubules. Clearly, these nanotubules are separately dispersed in the CS matrix and no bundles can be observed in the whole vision.

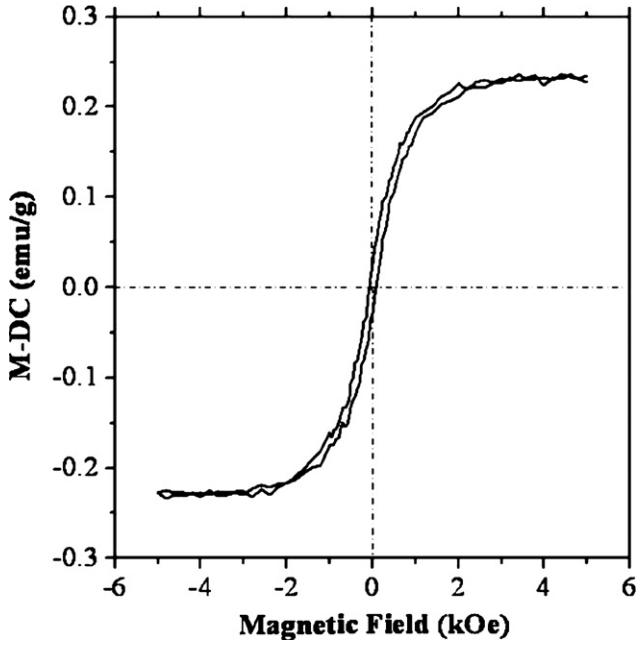

Fig. 3. Magnetization hysteresis loop for CS rod containing Fe_3O_4@PaPA/MWCNTs nanohybrid (measure at 298 K).

3.2. Alignment of Fe_3O_4@PaPA/MWCNTs nanostructures in CS matrix

The purpose of decorating Fe_3O_4 particles onto the surface of the PaPA/MWCNTs hybrid is to induce the alignment of the MWCNTs in the CS matrix by external magnetic field, thereby to enhance the bending strength and bending modulus of CS rods. To make sure the Fe_3O_4@PaPA/MWCNT nanohybrid can respond to the external magnetic filed, the coercivity and remanence of the Fe_3O_4@PaPA/MWCNTs nanohybrids were firstly evaluated by using a Quantum Design VSM with a field strength ranging from −5 to 5 kOe. The magnetization as a function of magnetic field strength is shown in Fig. 3. The magnetization of the sample rapidly increased with the increase of the field strength and became leveled off at ±2.2 kOe, and the saturation magnetization of the nanohybrid was ~0.23 emu/g. In addition, only very small hysteresis loop has been recorded. These behaviors indicate that the Fe_3O_4 nanoparticles are superparamagnetic materials. Meanwhile, a phase analysis was also conducted on an X-ray diffraction instrument, and the diffraction pattern is demonstrated in Fig. 4. The peak at 20.1° is the characteristic diffraction peak of CS. In comparison with the standard card [card no. 85-1436], the peaks at $2\theta = 35.6°$, 46.7°,

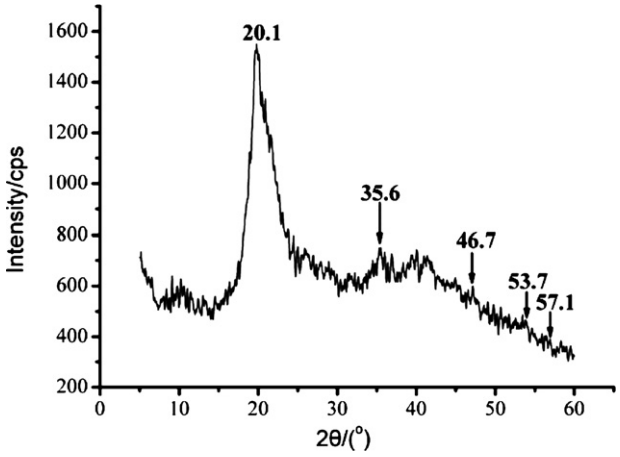

Fig. 4. X-ray diffraction pattern of the CS rod containing Fe_3O_4@PaPA/MWCNT nanohybrid.

and 53.7° are assigned to the diffractions from indices (3 1 1), (4 0 0), and (4 2 2), indicating that the Fe_3O_4 particles in the hybrid are pure Fe_3O_4 in a spinel polymorph (Wang, Bao, Yang, & Chen, 2008; Yan, Tomita, & Ikada, 1998). These data further confirm that the Fe_3O_4@PaPA/MWCNTs nanohybrid has the expected magnetic property.

To align the MWCNTs in CS matrix, a pair of permanent magnets was put at the two ends of the cylindrical mold during the *in situ* precipitation process. As shown in Scheme 2, upon the induction of the external magnetic field, the Fe_3O_4@PaPA/MWCNTs nanostructures gradually aligned in the axial direction of the cylindrical mold. This is confirmed by the TEM images given in Fig. 5. The ultra-thin slices were prepared as illustrated in Fig. 5A. Fig. 5B demonstrates the some typical morphological features of the slice sample. Firstly, several rod-like nano-sized entities with dark contrast can be observed; these entities are assigned to the Fe_3O_4@PaPA/MWCNTs due to the heavy Fe atoms and the background with light contrast is assigned to the CS matrix. Such an observation, together with the SEM image shown in Fig. 2, indicates that the Fe_3O_4@PaPA/MWCNTs nanohybrids have been incorporated into the CS matrix.

Secondly, the rod-like Fe_3O_4@PaPA/MWCNTs entities are aligned in the same direction with their long axis parallel to the axis of the rod, which can be judged from their respective alignment relative to the margin line of the slice sample. This observation validates the alignment of the Fe_3O_4@PaPA/MWCNTs nanohybrids in the resulted CS rods, which is induced by the applied magnetic field. Thirdly, Fig. 5C shows some details of the Fe_3O_4@PaPA/MWCNTs nanostructures; the areas marked with white arrows are the seg-

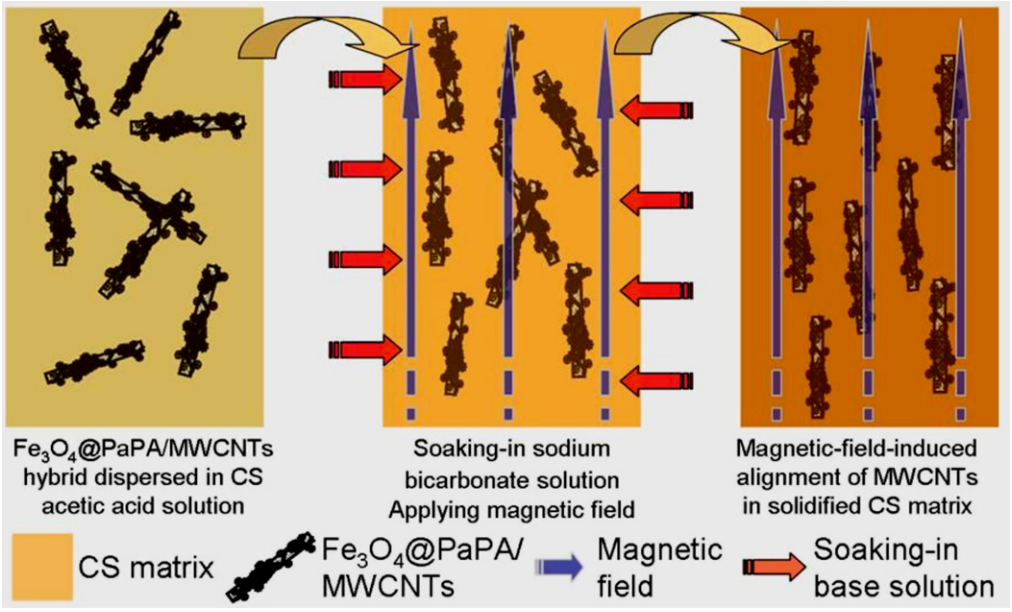

Scheme 2. Magnetic-field-induced alignment of Fe_3O_4@PaPA/MWCNTs nanostructures in CS matrix.

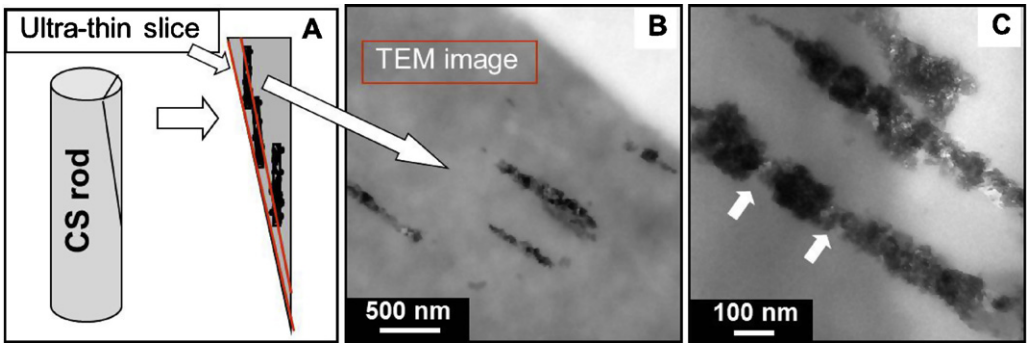

Fig. 5. (A) An illustration of the cutting of the ultrathin slices for TEM observation; (B) a typical TEM image of the ultrathin slice from a CS rod reinforced with Fe_3O_4@PaPA/MWCNTs nanohybrid; (C) a magnified image demonstrating the existence of partially "naked" MWCNTs (white arrows).

Table 2
Bending strength and bending modulus of different bone fracture internal fixation devices.[a]

Sample	Bending strength (MPa)	Bending modulus (GPa)
Pure CS rods	92.4 ± 2.0	4.1 ± 0.1
CS rods reinforced with nanohybrid of Fe_3O_4@PaPA/MWCNTs-1 (aligned)	109.4 ± 1.1	5.0 ± 0.1
CS rods reinforced with nanohybrid of Fe_3O_4@PaPA/MWCNTs-2 (aligned)	124.6 ± 1.3	5.3 ± 0.1
CS rods reinforced with nanohybrid of Fe_3O_4@PaPA/MWCNTs-2 (non-aligned)	96.0 ± 1.1	5.5 ± 0.1
Dikfix[b]	130.0	2.0–3.0
Biofix[b]	190.0–200.0	8.0–10.0

[a] Determined by using the standard method of ANSI/ASAE S459-1993. The data in the 1st and 2nd entries in the table are the average values of 5 parallel measurements.
[b] The data are extracted from Ref. (Hu et al., 2003).

ments decorated with Fe_3O_4 component, and the white arrows point at the "naked" or/and lightly decorated segments of the MWCNTs. These features imply the incomplete coverage of Fe_3O_4 on the surface of the PaPA/MWCNTs hybrids, consistent with the TEM micrograph in Fig. 1C. In addition, the length of the rod-like of Fe_3O_4@PaPA/MWCNTs nanostructures seems shorter than those observed in Fig. 1. This is due to the slicing operation in sample preparation (see Fig. 5A), which may cut off longer Fe_3O_4@PaPA/MWCNTs nanostructures.

3.3. Bending strength and modulus of the composite CS rods

The utmost goal of the present work is to enhance the bending strength and modulus of pure CS rods. To quantitatively evaluate the bending strength and modulus of the resulted CS rods containing Fe_3O_4@PaPA/MWCNTs nanohybrid, comparative experiments have been conducted on both pure and composite CS rods, and the data are list in Table 2. Also list in Table 2 are the reference data of a commercially available sample used for internal fixation of bone fracture (Dikfix Ltd., Co. and Biofix Ltd., Co.). Increasing the amount of Fe_3O_4@PaPA/MWCNTs led to higher mechanical properties. However, much more Fe_3O_4@PaPA/MWCNTs contained in CS solution resulted in much lower solution viscosity, and the mixture solution could not be prepared into CS rods, the detailed reason need further research. Bending strength and bending modulus of the CS rods reinforced with aligned nanohybrids could reach 124.6 MPa and 5.3 GPa, respectively. Quantitatively, these values increased by 34.8% and 29.3% in comparison with the pure CS rods. While in comparison with the CS rods blending with non-aligned nanohybrids, the bending strength increased 29.8%, while only lost 3.6% of the bending modulus. Especially, the bending strength is approximate to the quota of the nails made in Dikfix. The efficient improvement in the mechanical properties is associated with the good dispersion and aligned MWCNTs parallel to axis of the rods, which endure bending stress effectively.

Table 3
OD of control group and CS hybrid membranes group.

Groups	24 (h)	48 (h)	72 (h)
Control	1.008 ± 0.090	1.538 ± 0.091	1.675 ± 0.093
CS membranes containing Fe_3O_4@PaPA/ MWCNTs	0.490 ± 0.038	1.469 ± 0.064	2.296 ± 0.073

3.4. Cell proliferation on CS membrane containing Fe_3O_4@PaPA/MWCNTs nanohybrids

MG63 cells were cultivated with FBS DMEM, and then treated with Cell Titer 96 Aqueous One Solution Reagent (Promeg). The OD (A_{490}) of the CS hybrid membranes group and the control group is listed in Table 3. Compared with the control group, the CS hybrid membranes group could obviously promote MG63 cells proliferation ($P < 0.05$), so CS hybrid membranes containing Fe_3O_4@PaPA/MWCNTs are biocompatible and beneficial for the proliferation of cells.

4. Conclusions

We have fabricated composite CS rods reinforced with MWCNTs aligning in the axial direction of the cylindrical rod. The bending strength and bending modulus of the composite CS rods are 124.6 MPa and 5.3 GPa resepectively, which are 34.8% and 29.3% higher than the pure CS rods. These experimental results indicate that the key mechanical properties (bending strength and modulus) of the CS rods reinforced by axially aligned MWCNTs are approximate to the commercially available materials. The incorporation of the MWCNTs into CS matrix was achieved by simply mixing acidic aqueous CS solution and Fe_3O_4@PaPA/MWCNTs nanohybrids. The solubility of the Fe_3O_4@PaPA/MWCNTs in acidic aqueous solution derived from the protonated amino groups of the PaPA component. The alignment of the Fe_3O_4@PaPA/MWCNTs nanohybrid was realized by applying a magnetic field to the mixture solution during the *in situ* precipitation process. The response of the magnetic Fe_3O_4 particles to the external field ensured the orientation of the MWCNTs. SEM and TEM images, XRD and magnetization measurements confirmed the existence of magnetic Fe_3O_4@PaPA/MWCNTs nanohybrids in the prepared composite CS rods. In addition, it has been demonstrated that Fe_3O_4 is harmless to living tissues. For example, ferromagnetic bone cement is useful for local hyperthermia in bone (Wang et al., 2008; Yan et al., 1998). Sometimes, magnetism could stimulate bone growth (Markaki & Clyne, 2004; Takegami et al., 1998). CS-based biomaterials containing Fe_3O_4@PaPA/MWCNTs could obviously promote MG63 cells proliferation. Overall, the magnetic field assistant *in situ* precipitation method is facile to the preparation of CS rods. Therefore, the present work provides a useful strategy to fabricate different CS devices reinforced with various one-dimensional nanostructures.

Acknowledgements

The work reported in this paper was partially supported by the National Natural Science Foundation of China (50773070, 20634020, 50740460164), the Key Basic Research Development Plan of China (grant no. 2009CB930104), China Postdoctoral Science Foundation (20100480085) and Grand Science and Technology Special Project of Zhejiang Province (grant no. 2008C11087). B.Z.T. thanks the support from Cao Guangbiao Foundation of Zhejiang University. The authors thank Jieru Wang and Yin Xu for their kind supports in SEM and TEM analysis.

References

Chen, F. P., Hu, Q. L., Chen, L., Li, B. Q., & Shen, J. C. (2006). Preparation of magnetic iron oxide/hydroxyapatite/cbtirosan rods by in situ precipitation. *Acta Polymerica Sinica*, *6*, 756–760.
Di Martino, A., Sittinger, M., & Risbud, M. V. (2005). Chitosan: A versatile biopolymer for orthopaedic tissue-engineering. *Biomaterials*, *26*, 5983–5990.
Dou, S. X., Yeoh, W. K., Shcherbakova, O., Weyler, D., Li, Y., Ren, Z. M., et al. (2006). Alignment of carbon nanotube additives for improved performance of magnesium diboride superconductors. *Advanced Materials*, *18*, 785–788.
Dresselhaus, M. S., Dresselhaus, G., & Eklund, P. C. (1996). *Science of fullerenes & carbon nanotubes*. San Diego: Academic Press.

Gupta, K. C., & Jabrail, F. H. (2006). Preparation and characterization of sodium hexameta phosphate cross-linked chitosan microspheres for controlled and sustained delivery of centchroman. *International Journal of Biological Macromolecules*, *38*, 272–283.

Hu, Q. L., Chen, F. P., Li, B. Q., & Shen, J. C. (2006). Preparation of three-dimensional nano-magnetite/chitosan rod. *Materials Letters*, *60*, 368–370.

Hu, Q. L., Li, B. Q., Wang, M., & Shen, J. C. (2004). Preparation and characterization of biodegradable chitosan/hydroxyapatite nanocomposite rods via in situ hybridization: A potential material as internal fixation of bone fracture. *Biomaterials*, *25*, 779–785.

Hu, Q. L., Qian, X. Z., Li, B. Q., & Shen, J. C. (2003). Studies on chitosan rods prepared by in situ precipitation method. *Chemical Journal of Chinese Universities-Chinese*, *24*, 528–531.

Hu, W. J., He, X. Y., Deng, Y. J., Xie, F., Liu, X. Y., & Chen, M. J. (2002). A clinical study on DIKFIX absorbable internal fixation screws. *Chinese Journal of Orthopaedic Trauma*, *4*, 258–259.

Hussain, S. M., Braydich-Stolle, L. K., Schrand, A. M., Murdock, R. C., Yu, K. O., Mattie, D. M., et al. (2009). Toxicity evaluation for safe use of nanomaterials: Recent achievements and technical challenges. *Advanced Materials*, *21*, 1549–1559.

Islam, M. F., Rojas, E., Bergey, D. M., Johnson, A. T., & Yodh, A. G. (2003). High weight fraction surfactant solubilization of single-wall carbon nanotubes in water. *Nano Letters*, *3*, 269–273.

Kang, Y. K., Lee, O. S., Deria, P., Kim, S. H., Park, T. H., Bonnell, D. A., et al. (2009). Helical wrapping of single-walled carbon nanotubes by water soluble poly(*p*-phenyleneethynylene). *Nano Letters*, *9*, 1414–1418.

Kharisov, B. I., Kharissova, O. V., Gutierrez, H. L., & Mendez, U. O. (2009). Recent advances on the soluble carbon nanotubes. *Industrial & Engineering Chemistry Research*, *48*, 572–590.

Kim, S., Xuan, Y., Ye, P. D., Mohammadi, S., & Lee, S. W. (2008). Single-walled carbon nanotube transistors fabricated by advanced alignment techniques utilizing CVD growth and dielectrophoresis. *Solid State Electronics*, *52*, 1260–1263.

Kim, S. B., Kim, Y. J., Yoon, T. R., Park, S. A., Cho, I. H., Kim, E. J., et al. (2004). The characteristics of a hydroxyapatite–chitosan–PMMA bone cement. *Biomaterials*, *25*, 5715–5723.

Kim, S. K., Lee, H. W., Tanaka, H., & Weiss, P. S. (2008). Vertical alignment of single-walled carbon nanotube films formed by electrophoretic deposition. *Langmuir*, *24*, 12936–12942.

Kumar, S., & Bisoyi, H. K. (2007). Aligned carbon nanotubes in the supramolecular order of discotic liquid crystals. *Angewandte Chemie International Edition*, *46*, 1501–1503.

Lagerwall, J., Scalia, G., Haluska, M., Dettlaff-Weglikowska, U., Roth, S., & Giesselmann, F. (2007). Nanotube alignment using lyotropic liquid crystals. *Advanced Materials*, *19*, 359–364.

Lee, S. W., Kim, B. S., Chen, S., Shao-Horn, Y., & Hammond, P. T. (2009). Layer-by-layer assembly of all carbon nanotube ultrathin films for electrochemical applications. *Journal of the American Chemical Society*, *131*, 671–679.

Leroux, L., Hatim, Z., Freche, M., & Lacout, J. L. (1999). Effects of various adjuvants (lactic acid, glycerol, and chitosan) on the injectability of a calcium phosphate cement. *Bone*, *25*, 31–34.

Lu, Y. L., Cheng, C. M., Leduc, P. R., & Ho, M. S. (2008). Controlling the mechanics and nanotopography of biocompatible scaffolds through dielectrophoresis with carbon nanotubes. *Electrophoresis*, *29*, 3123–3127.

MacNeil, S. (2008). Biomaterials for tissue engineering of skin. *Materials Today*, *11*, 26–35.

Markaki, A. E., & Clyne, T. W. (2004). Magneto-mechanical stimulation of bone growth in a bonded array of ferromagnetic fibres. *Biomaterials*, *25*, 4805–4815.

Matarredona, O., Rhoads, H., Li, Z. R., Harwell, J. H., Balzano, L., & Resasco, D. E. (2003). Dispersion of single-walled carbon nanotubes in aqueous solutions of the anionic surfactant NaDDBS. *Journal of Physical Chemistry B*, *107*, 13357–13367.

Miaudet, P., Badaire, S., Maugey, M., Derre, A., Pichot, V., Launois, P., et al. (2005). Hot-drawing of single and multiwall carbon nanotube fibers for high toughness and alignment. *Nano Letters*, *5*, 2212–2215.

Moroni, L., & Elisseeff, J. H. (2008). Biomaterials engineered for integration. *Materials Today*, *11*, 44–51.

Narita, N., Kobayashi, Y., Nakamura, H., Maeda, K., Ishihara, A., Mizoguchi, T., et al. (2009). Multiwalled carbon nanotubes specifically inhibit osteoclast differentiation and function. *Nano Letters*, *9*, 1406–1413.

Nel, A. E., Madler, L., Velegol, D., Xia, T., Hoek, E. M. V., Somasundaran, P., et al. (2009). Understanding biophysicochemical interactions at the nano-bio interface. *Nature Materials*, *8*, 543–557.

Peng, X. H., & Wong, S. S. (2009). Functional covalent chemistry of carbon nanotube surfaces. *Advanced Materials*, *21*, 625–642.

Saito, N., Usui, Y., Aoki, K., Narita, N., Shimizu, M., Hara, K., et al. (2009). Carbon nanotubes: Biomaterial applications. *Chemical Society Reviews*, *38*, 1897–1903.

Saito, N., Usui, Y., Aoki, K., Narita, N., Shimizu, M., Ogiwara, N., et al. (2008). Carbon nanotubes for biomaterials in contact with bone. *Current Medicinal Chemistry*, *15*, 523–527.

Saito, R., Dresselhaus, M. S., & Dresselhaus, G. (1998). *Physical properties of carbon nanotubes*. London: Imperial College Press.

Salhi, F., Cheuk, K. K. L., Sun, Q. H., Lam, J. W. Y., Cha, J. A. K., Li, G., et al. (2001). Rapid fabrication of three-dimensional porous films with biomimetic patterns by natural evaporation of amphiphilic polyacetylene solutions under ambient conditions. *Journal of Nanoscience and Nanotechnology*, *1*, 137–141.

Scalia, G., von Buhler, C., Hagele, C., Roth, S., Giesselmann, F., & Lagerwall, J. P. F. (2008). Spontaneous macroscopic carbon nanotube alignment via colloidal suspension in hexagonal columnar lyotropic liquid crystals. *Soft Matter*, *4*, 570–576.

Sirivisoot, S., & Webster, T. J. (2008). Multiwalled carbon nanotubes enhance electrochemical properties of titanium to determine in situ bone formation. *Nanotechnology*, *19*, 295101.

Takegami, K., Sano, T., Wakabayashi, H., Sonoda, J., Yamazaki, T., Morita, S., et al. (1998). New ferromagnetic bone cement for local hyperthermia. *Journal of Biomedical Materials Research*, *43*, 210–214.

Tang, B. Z., & Xu, H. Y. (1999). Preparation, alignment, and optical properties of soluble poly(phenylacetylene)-wrapped carbon nanotubes. *Macromolecules*, *32*, 2569–2576.

Tumpane, J., Karousis, N., Tagmatarchis, N., & Norden, B. (2008). Alignment of carbon nanotubes in weak magnetic fields. *Angewandte Chemie International Edition*, *47*, 5148–5152.

Veetil, J. V., & Ye, K. M. (2009). Tailored carbon nanotubes for tissue engineering applications. *Biotechnology Progress*, *25*, 709–721.

Wang, S., Bao, H. M., Yang, P. Y., & Chen, G. (2008). Immobilization of trypsin in polyaniline-coated nano-Fe3O4/carbon nanotube composite for protein digestion. *Analytica Chimica Acta*, *612*, 182–189.

Xu, H. P., Jin, J. K., Mao, Y., Sun, J. Z., Yang, F., Yuan, W. Z., et al. (2008). Synthesis of sulfur-containing polyacetylenes and fabrication of their hybrids with ZnO nanoparticles. *Macromolecules*, *41*, 3874–3883.

Xu, H. P., Mao, Y., Yuan, W. Z., Sun, J. Z., Dong, Y. Q., Wang, M., et al. (2007). Solubility improvement and surface functionalization of multi-walled carbon nanotubes by a thiol-functionalized poly (phenylacetylene) derivative. *Acta Polymerica Sinica*, *52*, 897–900.

Xu, J. L., Khor, K. A., Sui, J. J., & Chen, W. N. (2009). Preparation and characterization of a novel hydroxyapatite/carbon nanotubes composite and its interaction with osteoblast-like cells. *Materials Science & Engineering C-Biomimetic and Supramolecular Systems*, *29*, 44–49.

Yan, Q. C., Tomita, N., & Ikada, Y. (1998). Effects of static magnetic field on bone formation of rat femurs. *Medical Engineering & Physics*, *20*, 397–402.

Yuan, W. Z., Sun, J. Z., Dong, Y. Q., Haussler, M., Yang, F., Xu, H. P., et al. (2006). Wrapping carbon nanotubes in pyrene-containing poly(phenylacetylene) chains: Solubility, stability, light emission, and surface photovoltaic properties. *Macromolecules*, *39*, 8011–8020.

Yuan, W. Z., Tang, L., Zhao, H., Jin, J. K., Sun, J. Z., Qin, A. J., et al. (2009). Direct polymerization of highly polar acetylene derivatives and facile fabrication of nanoparticle-decorated carbon nanotubes. *Macromolecules*, *42*, 52–61.

Yuan, W. Z., Zhao, H., Xu, H. P., Sun, J. Z., Lam, J. W. Y., Mao, Y., et al. (2007). Improvement of the solubility of multiwalled carbon nanotubes with disubstituted polyacetylenes bearing different side-chains. *Acta Polymerica Sinica*, *10*, 901–904.

Yurekli, K., Mitchell, C. A., & Krishnamoorti, R. (2004). Small-angle neutron scattering from surfactant-assisted aqueous dispersions of carbon nanotubes. *Journal of the American Chemical Society*, *126*, 9902–9903.

Zhao, H., Yuan, W. Z., Mei, J., Tang, L., Liu, X. Q., Yan, M., et al. (2009). Enhanced dispersion of nanotubes in organic solvents by donor–acceptor interaction between functionalized poly(phenylacetylene) chains and carbon nanotube walls. *Journal of Polymer Science A: Polymer Chemistry*, *19*, 4995–5005.

Zhao, H., Yuan, W. Z., Tang, L., Sun, J. Z., Xu, H. P., Qin, A. J., et al. (2008). Hybrids of triphenylamine-functionalized polyacetylenes and multiwalled carbon nanotubes: High solubility, strong donor–acceptor interaction, and excellent photoconductivity. *Macromolecules*, *41*, 8566–8574.

Zhu, Y., Wang, X. H., Cui, F. Z., Feng, Q. L., & De Groot, K. (2003). In vitro cytocompatibility and osteoinduction of phosphorylated chitosan with osteoblasts. *Journal of Bioactive and Compatible Polymers*, *18*, 375–390.